Reactions of Phospholipase A_2 at a Mercury Electrode Surface

Shaowei Chen and Héctor D. Abruña*

Department of Chemistry, Baker Laboratory, Cornell University, Ithaca, New York 14853-1301

Received: March 19, 1996; In Final Form: October 21, 1996[⊗]

Cyclic voltammetric techniques (dc and ac) have been employed to probe the interfacial interaction of porcine pancreatic phospholipase A_2 (PLA_2) with mercury. A reaction mechanism based on the interaction of cystine residues (disulfide) with mercury is presented. It appears that the interfacial electrical properties play an important role in determining the surface behavior of adsorbed PLA_2 molecules. For instance, the predominant step of the electron transfer process is dependent on the electrode surface properties, including the surface concentration of PLA_2 and the fraction of free surface mercury sites. In addition, the local pH at the interface and interfacial buffer capacity were also found to be important factors in the surface reaction mechanism. Studies of the electron transfer kinetics showed that the transfer coefficient (α) was somewhat less than 0.50, and the rate constant (k) was of the order of 10^3 s^{-1}. From ac cyclic voltammetric studies it was determined that the adsorbed PLA_2 layer corresponded to a capacitor of about 6 μF/cm^2 and that the faradaic component of the interfacial capacitance was about 1 μF/cm^2.

Introduction

There has been much interest in studying the interfacial reactions of thiols/disulfides at noble metal electrode surfaces, such as gold,[1] silver,[2] and platinum[3] as well as mercury.[4−6] It is generally found that thiols/disulfides adsorb very strongly to these metal surfaces and that the adsorption involves rather complicated surface reactions, mainly due to the fact that the sulfur functional groups readily react with these metal centers to form the corresponding, and energetically more stable, thiolate complexes. Such reactions enhance the adsorption of the molecules in turn, typifying the surface behavior of this group of molecules. Among these studies, those on the cystine/cysteine system on mercury electrode surfaces[6] are particularly valuable in terms of providing insight into the surface reaction mechanism. Since both cystine and cysteine show rather well-defined electrochemical responses, electrochemical techniques have been quite extensively employed in addressing the above-mentioned problems. On the basis of the studies of cystine/cysteine on mercury electrode surfaces,[6] it has been postulated that the reaction series consists of the essential step of formation of a mercury thiolate complex (chemisorption) prior to the actual electron transfer process (electrochemical reaction) (Scheme 1), which is summarized below:

$$RSSR + Hg \leftrightarrows (RS)_2Hg_{(ads)} \quad (1)$$

$$(RS)_2Hg_{(ads)} + Hg \leftrightarrows 2RSHg_{(ads)} \quad (2)$$

$$(RS)_2Hg_{(ads)} + 2H^+ + 2e^- \leftrightarrows 2RSH_{(ps)} + Hg \quad (3)$$

$$RSHg_{(ads)} + H^+ + e^- \leftrightarrows RSH_{(ps)} + Hg \quad (4)$$

where the subscript (ads) denotes adsorption through a thiolate linkage and (ps) denotes a physisorbed and/or adsorbed state through interactions different from a thiolate. We make this distinction to differentiate molecules adsorbed via thiolate/mercury interactions from other types of interactions that are likely present in this case such as intermolecular and chain/chain interactions. However, as to which reaction is the actual rate-determining step, it is postulated that either of the surface reactions of the disulfide group with mercury as shown in (1) and (2) can be the slow, rate-limiting step. In a previous study[7] we have demonstrated that the rate constant of PLA_2 adsorption onto mercury via one of its seven disulfide groups is of the order of 10^4 s^{-1}, indicating that in this case reaction 1 is fairly rapid. Thus, it is likely that in PLA_2 adsorption the actual rate-limiting step is the disulfide bond-breaking/bond-forming reaction, as shown in (2). On the other hand, as shown in the above

SCHEME 1: Schematic Depiction of the Surface Reaction Mechanism of a Disulfide Group on a Mercury Surface[a]

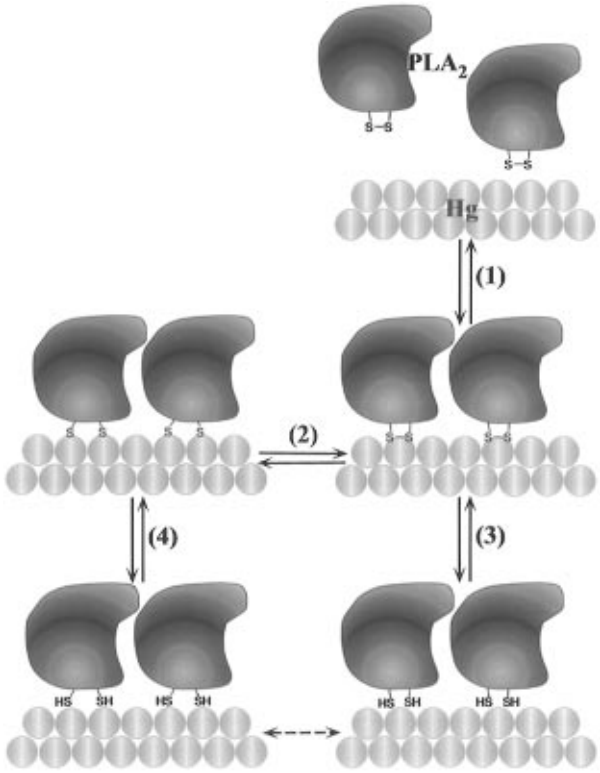

[a] Reaction steps correspond to those indicated in the text. Although PLA_2 is used as an example, the scheme can be used for other disulfide species. Note that the figure is not to scale.

[⊗] Abstract published in *Advance ACS Abstracts,* December 15, 1996.

S1089-5647(96)00837-1 CCC: $14.00

reaction scheme, there is a coexistence of mercury(I) and -(II) thiolate complexes, which apparently depends on the specific surface conditions, such as the concentrations of disulfide and mercury (i.e., the concentration of free surface mercury). Correspondingly, there are two electron transfer pathways, (3) and (4), which involve two protons/two electrons and one proton/one electron, respectively.

It has been previously demonstrated that the electrical properties of the interface play an important role in the above-mentioned reaction mechanism of cystine/cysteine,[6] and one would anticipate that a similarly important role would be played in the reactions of disulfide groups within enzymes. This provides, in part, our motivation for the study of the interfacial reactions of one of the disulfide groups within the hydrolytic enzyme PLA_2 since it may provide additional insight on the interfacial reactivity of thiols/disulfides systems within enzymes, especially since the bulky physical size and amphiphilic molecular nature of PLA_2 are believed to affect dramatically its interfacial properties, such as charge/potential distribution, solvation, and others. Since these properties are often correlated with the reactivity and the mechanism of the enzymatic reaction, we would anticipate that these would be affected as well and consequently our interest in their study and characterization. Moreover, we are interested in developing new electrochemical methodologies for the determination of interfacial enzymatic activity of enzymes such as PLA_2 whose activity is a strong function of its state of aggregation at interfaces. In order to develop such methodologies, an understanding of the reactivity of PLA_2 at electrochemical interfaces is a necessary and key initial step and this provides an additional incentive for their study.

We recently carried out some studies on the adsorption dynamics of porcine pancreatic phospholipase A_2 (PLA_2) onto a hanging mercury drop electrode (HMDE) surface.[7] Since this study suggested that the adsorption was through a cystine residue within the enzyme, we wanted to probe the surface reactions involved, thereby providing additional insight into the current understanding of the thiol/disulfide chemisorption. We have carried out additional studies of this system with both dc and ac cyclic voltammetric techniques, in terms of the surface reaction mechanism, electron transfer kinetics, and the electrical properties of the adsorbed PLA_2 molecules.

Experimental Section

Materials. Phospholipase A_2 (PLA_2) from pig pancreas, which was originally suspended in 3.2 M $(NH_4)_2SO_4$ solution (pH 5.4) at a concentration of 6.3 mg/mL, was obtained from Sigma and used as received. Electrolyte solutions were prepared with ultrapure salts (Aldrich) which were at least of 99.99+% purity. These salts were dissolved (0.20 M) in water which was purified with a Millipore Milli-Q system and buffered with phosphate salts (Aldrich, 99+%), tris(hydroxymethyl)amino-methane (TRIS, from Sigma, 99.0−99.5%), and hydrochloric acid (Aldrich, 99.999%) depending on the desired pH.

Apparatus. The experimental apparatus and data analysis for dc cyclic voltammetry have been described previously.[7] In the ac voltammetry experiments, the sine wave was generated with a Tektronix CFG 250 function generator, with a typical frequency of 73 Hz and a peak-to-peak amplitude of 10 mV. This ac signal was superimposed onto a 10 mV/s dc ramp which was generated with an EG&G PARC Model 175 universal programmer. The resulting signals were fed to an EG&G Model 173 potentiostat, coupled to an EG&G lock-in amplifier (Model 5209), from which the out-of-phase (90°) signals were recorded with a Hewlett-Packard 7045B $X-Y$ recorder.

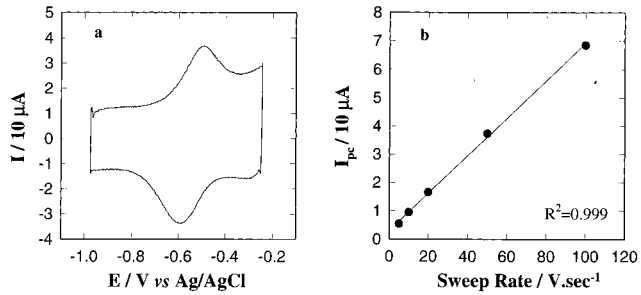

Figure 1. (a) Cyclic voltammogram of PLA_2 adsorbed onto a mercury electrode in 0.20 M KCl buffered with 0.010 M $K_2HPO_4-KH_2PO_4$ (pH 6.7). Sweep rate 50 = V/s, electrode surface area = 1.82 mm^2, and PLA_2 concentration = 0.030 μM. (b) Cathodic peak current vs sweep rate.

Simulations were carried out using Digi-Sim 2.1 (Bioanalytical Systems).

Procedure. The experimental procedure has been described previously;[7] i.e., the time evolution of the adsorption of PLA_2 onto a mercury electrode was followed by holding the potential at −0.25 or −0.30 V and taking cyclic voltammetric scans at various time intervals (shorter at the beginning and longer at the end).

Results and Discussions

Surface Reaction Mechanism. *(a) Adsorbed States of PLA_2.* In our previous study on the adsorption dynamics,[7] we showed that the typical electrochemical response for PLA_2 adsorbed onto a mercury electrode surface is that presented in Figure 1, where one can see a pair of well-defined voltammetric waves (Figure 1a) whose peak currents were directly proportional to the sweep rate (Figure 1b), indicating that they are due to an electrochemical reaction involving adsorbed species. This redox response was ascribed to the reduction/oxidation of one of the disulfide bonds of the cystine residues in the enzyme adsorbed onto the mercury surface. The overall electrochemical reaction can be represented as

$$RSSR + 2H^+ + 2e^- \leftrightarrow 2RSH \qquad (5)$$

In contrast to the experimental value of 71 mV,[7] this reaction would be expected to exhibit a 59 mV shift of the formal potential (at 25 °C) per pH unit change as predicted by the Nernst equation. As to the origin of this difference, it was difficult to ascertain without a better understanding of the reaction mechanism (more detailed discussion below).

Figure 2a shows the cyclic voltammograms of PLA_2 adsorption while Figure 2b presents the variation of the corresponding peak and formal potentials with time. It can be seen that there are quite significant shifts in the peak potentials during the adsorption process, i.e., with increasing surface coverage of PLA_2. As more PLA_2 is adsorbed onto the electrode surface, both cathodic and anodic peak potentials shift positively, by up to 100 mV. Once a saturated surface coverage is reached, the anodic peak potential remains practically unchanged while the cathodic peak potential reaches a local maximum and then shifts more slowly into an also constant value. Here it should be noted that the shift of the anodic peak potentials was always much greater than that of the cathodic peak potential, indicating that the reduced form is more strongly adsorbed which is consistent with the presence of two thiols relative to a disulfide. These observations are consistent with the above-mentioned reaction scheme. In the case of the cystine/cysteine system, at the early stages of adsorption, since there is an excess of free mercury, this will facilitate reactions 1 and 2 with the final

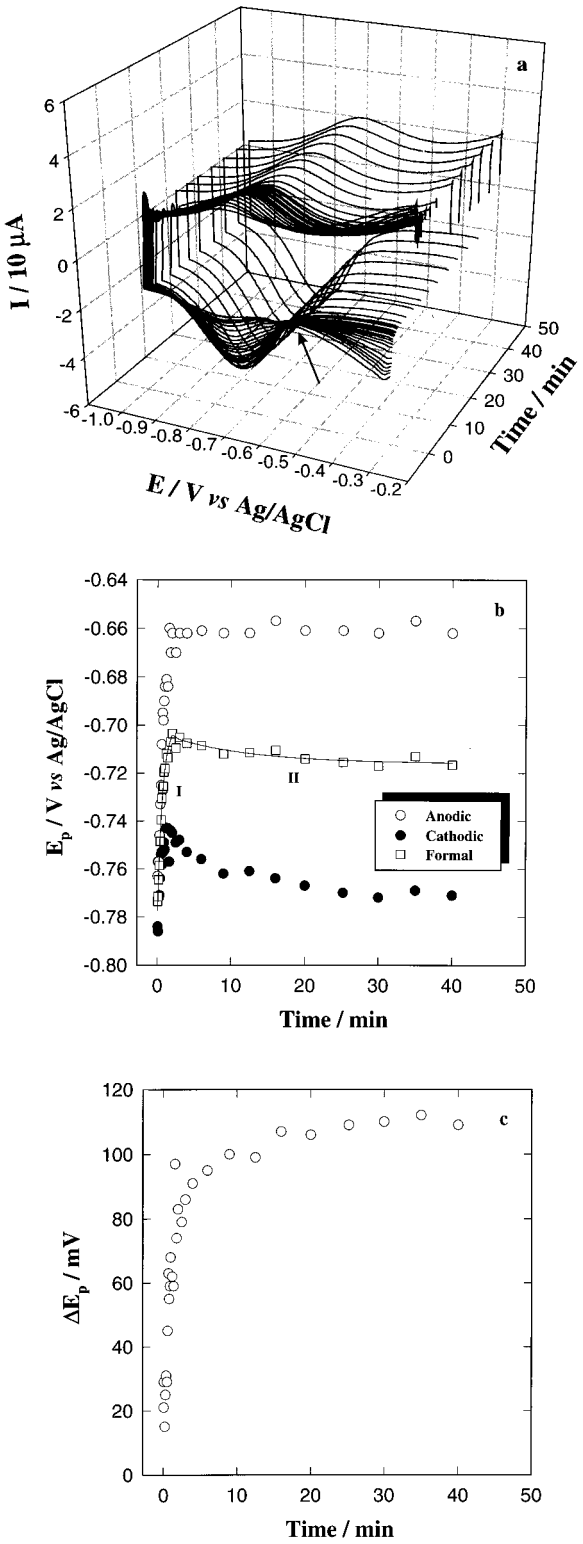

Figure 2. (a) Three-dimensional plot of cyclic voltammograms with time of PLA_2 adsorption onto a mercury electrode in 0.20 M KCl buffered with 0.010 M Tris-HCl (pH 8.6). Other experimental conditions were the same as in Figure 1. Arrow indicates isopotential point. (b) Peak potentials of the cathodic and anodic waves during the adsorption process. (c) Difference of peak potentials vs adsorption time.

formation of RSHg, whereas with an increase in coverage, the formation of $(RS)_2Hg$ is favored.[6] However, in the present case of phospholipase A_2, because of its bulky physical size, it is likely that the mechanism is more complex and/or different from that of the cystine/cysteine system. Here one should also recall that, during the PLA_2 adsorption process, the electrode was held at −0.25 or −0.30 V, which is quite positive of the disulfide

SCHEME 2: Schematic Illustrations of the Variations of the Adsorbed Forms of PLA_2 onto a Mercury Surface Depending on the Adsorption Stage[a]

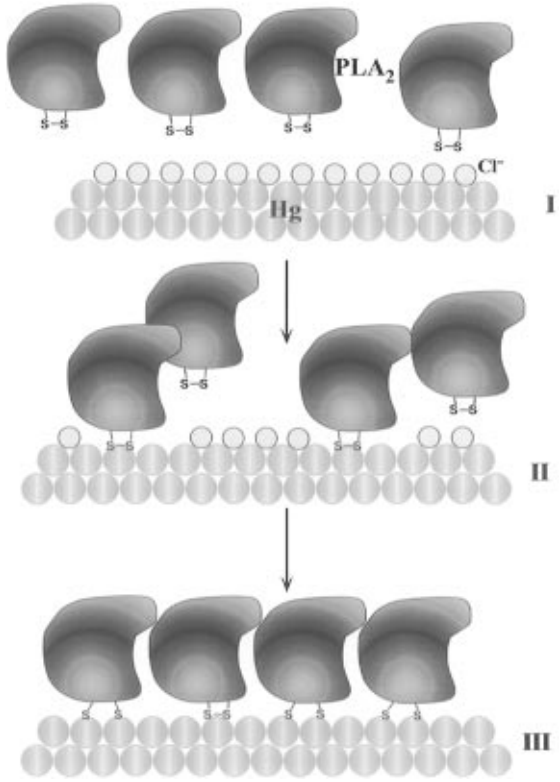

[a] I, initial stage; II, partial coverage of the electrode surface; III, final full coverage stage of adsorbed PLA_2 on the mercury electrode surface.

redox formal potential under the same experimental conditions. As this electrode potential is also positive of the corresponding potential of zero charge (PZC) for chloride on mercury,[8] there is in all likelihood a preadsorbed layer of chloride anions on the electrode surface, due to specific adsorption (Scheme 2, stage I). Therefore, the adsorption of PLA_2 is accompanied by the concomitant displacement of adsorbed chloride from the electrode surface (stage II), which is also suggested by the isopotential points in the cyclic voltammograms (Figure 2a). At the early stages of adsorption, adsorbed PLA_2 molecules are surrounded by chloride anions, which compete with PLA_2 molecules for surface mercury sites (stage II). Hence, due to the limited access to surface free mercury, it is most likely that the adsorbed form of PLA_2 is $(RS)_2Hg$, which would also be the electroactive species that undergoes reversible electron transfer. As more PLA_2 molecules are adsorbed onto the electrode surface, more chloride anions are expelled (desorbed) from the surface. Thus, adsorbed PLA_2 could have access to additional free surface mercury and react further to form RSHg (stage III). Taking into account the above observations, one could speculate that there might be different predominating electron transfer pathways depending upon the surface concentrations of adsorbate and mercury, i.e., (3) and (4) during the initial and final stages, respectively. In their cathodic reactions, $(RS)_2Hg$ and RSHg are reduced by two protons/two electrons and one proton/one electron, respectively. However, one should note that in (3) the two thiol groups were bound to the same mercury while in (4) it involves two different mercury sites. Hence, one would expect that reaction 3 would be energetically less favorable than (4). On the other hand, the anodic reaction involves the restoration of the disulfide bond (4), which would be expected to be kinetically more sluggish than (3) since it

requires that the two adsorbed thiols move onto the same mercury by a distance of about 1.2 Å, taking into account the bond lengths of mercury−mercury and sulfur−sulfur.[8]

The formal potential ($E^{\circ\prime}$) reflects the relative energetic states of the reactants and products in an electrochemical process in terms of the overall Gibbs free energy change

$$\Delta G = -nFE^{\circ\prime} \tag{6}$$

where ΔG is the free energy change, $E^{\circ\prime}$ is the formal potential, F is Faraday's constant, and n is the number of electrons transferred. It can be seen that when $E^{\circ\prime}$ shifts positively, ΔG becomes more negative, indicating that the process is energetically more facile. This is consistent with the above argument that the adsorbed form of PLA_2 developed, from $(RS)_2Hg$ at the early stages, to subsequently form RSHg at higher surface coverage, since the former involves a bond-breaking step in addition to the electron transfer process, in contrast to the latter case. The shift of $E^{\circ\prime}$ with increasing coverage would also suggest that adsorbed PLA_2 molecules are initially randomly distributed and subsequently aggregate into clusters/islands, such that the local environment and consequently the energetic state of the adsorbed molecules would be altered during this aggregation process.

Since, as mentioned above, during the adsorption process there appear to be two different electron transfer pathways, there would ostensibly be two different formal potentials one associated with each pathway, respectively. However, we have found that the potential separation between these two processes is small (vide infra) so that what one would measure experimentally would be some average (likely the weighted average) of these two reactions which will, in turn, depend on coverage (time). At time t, the surface coverage would be Γ_t, from which a fraction, $1 - x$, would be in the form of $(RS)_2Hg$ and $2x$ in the form of RSHg. The apparent formal potential, $E^{\circ\prime}$, could be expressed as

$$E^{\circ\prime} = (1 - x)E_3 + xE_4 \tag{7}$$

where E_3 and E_4 are the formal potentials for reactions 3 and 4, respectively. We recognize that eq 7 is neither thermodynamically rigorous nor formally correct. Rather, we use it in a phenomenological way to describe the experimental results. That such a treatment can qualitatively describe the experimental behavior can be shown by running simple simulations for two closely spaced surface-confined redox processes at constant total coverage. We have, in fact, carried out such a simulation (data not shown) using the program Digi-Sim (Bioanalytical Systems) where it can be clearly observed that as the relative coverage of the two components changes, the peak potential shifts in qualitatively the same way as was observed experimentally. We reiterate that we are aware of the limitations of eq 7 but also note that it provides some qualitative information.

Equation 7 can also be recast as

$$E^{\circ\prime} = E_3 + x(E_4 - E_3) \tag{8}$$

As E_3 and E_4 are both constants, the dependence of $E^{\circ\prime}$ on time is implied in x. Figure 2b shows the fitting of the formal potential vs time, where it can be seen that there is a two-phase transition of the formal potential, designated as I and II, respectively, both of which are fit quite well by a simple exponential expression, $E^{\circ\prime} = a + be^{-kt}$. The fitting parameters are shown in Table 1, where it can be seen that the rate constant for phase I is about 15-fold greater than that for phase II (phase II might suggest a relaxation process). Taking into account eq 8, one can get

TABLE 1: Fitting Parameters for the Shift in the Formal Potential, $E^{\circ\prime}$, of PLA_2

	a^a (V)	b^a (V)	k (min^{-1})
phase I	-0.700 ± 0.003	-0.083 ± 0.003	1.50 ± 0.14
phase II	-0.716 ± 0.001	0.0132 ± 0.002	0.09 ± 0.04

[a] All potentials are referred to the reference electrode, Ag/AgCl saturated with NaCl.

$$x = \frac{a - E_3}{E_4 - E_3} + \frac{b}{E_4 - E_3}\, e^{-kt} \tag{9}$$

which clearly shows an exponential dependence of the partition of the adsorbed PLA_2 molecules between the mercury(I) and -(II) complexes. As $E_4 > E_3$, which is implied in the relative energetic states of $(RS)_2Hg$ and RSHg, and in phase I, $b < 0$ (Table 1), then x increases with increasing t. This is consistent with our earlier argument that, with increasing surface coverage, the predominant adsorbed form of PLA_2 is RSHg.

If we assume that when $t = 0$, $x = 0$, i.e., at the initial stage of adsorption, $(RS)_2Hg$ is the predominant form, then from eq 9 one can get that $E_3 = a + b$. From the fitting results, $a = -0.700$ and $b = -0.083$; thus $E_3 = -0.783$ V vs Ag/AgCl. However, at the present time we are not certain that at the final stages of adsorption 100% of the adsorbed molecules are in the form of RSHg. Thus, we can only estimate the lower limit for E_4, which is reflected in the peak of the curve, $E_4 \geq -0.704$ V (Figure 2b). There is a potential difference of these two reactions of only about 80 mV, corresponding to an energy difference of about 15 kJ/mol. One can see that the overall energetic difference between these two adsorbed forms is not very significant. This might be due to the fact that although one involves the breaking of a disulfide bond, it is compensated by the formation of two Hg(I)−S bonds.

Figure 2c shows the difference in peak potentials (ΔE_p) with time. One can note that ΔE_p increases with increasing time (coverage), reflecting a decrease in the degree of reversibility of the related electrochemical reactions. On the basis of the reaction scheme (Scheme A) described above, we believe that these observations can be interpreted, at least in part, in terms of the interfacial availability of protons which are necessary for the redox reactions. At the early stages, with only very low surface coverage of PLA_2, protons can readily reach the redox active site of the adsorbate, whereas as the surface coverage increases, the adsorbed molecules become more compact; hence, the energetic barrier for protons to diffuse to the interface is increased. Given that the redox events involve protons, their availability would be anticipated to be reflected in the kinetics. Additional effects of protons on these reactions will be discussed further below and in section b.

It is instructive to compare the very first voltammetric scan (at high sweep rate, e.g., 50 V/s) to subsequent ones for a saturated surface. As shown in Figure 3, one can see that the cathodic wave peak current of the very first cycle is significantly greater than those of the subsequent scans, which are almost constant, while the anodic peak currents remain virtually unchanged throughout. Also, the difference between the first and the subsequent cycles of the cathodic scans is dependent upon the sweep rate: the higher the sweep rate, the greater the difference. This behavior is also consistent with the above argument that the supply of protons to the interface could, in part, account for the observed responses. In addition, the decrease of the cathodic wave in subsequent scans might indicate

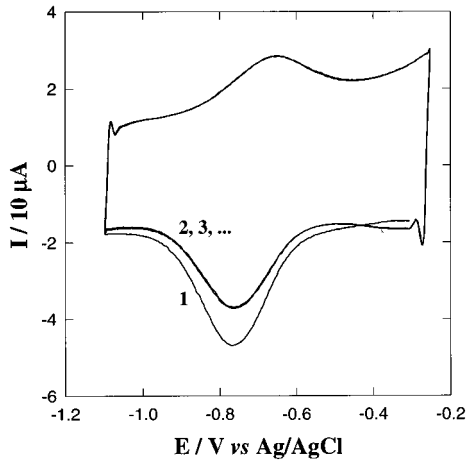

Figure 3. Cyclic voltammograms of the steady state of PLA_2 adsorbed on a mercury electrode surface. Experimental conditions were the same as in Figure 2. Numbers shown represent the scan number.

that due to the compact aggregation of the adsorbed film and geometric constraints, the reoxidation of RSH back to RSSR is not complete, as suggested above.[6] This is also consistent with the observation that, in the early stages of adsorption, the cathodic and anodic waves were almost equal in height.

(b) Effect of pH in the Local Microenvironment. To further probe the surface reaction, we also carried out an experiment where the supporting electrolyte (0.20 M KCl) was not buffered and the bulk pH was around 5. Figure 4a shows the corresponding electrochemical responses, where it can be seen that the reversibility of the overall reaction was dramatically decreased with the anodic wave almost completely disappearing. From the peak position of the cathodic wave it was estimated that the responses were very similar to those at pH 8−9. Thus, it appears that the adsorbed PLA_2 is itself able to adjust the pH in its vicinity (local pH) due to its multiple protonable groups around the adsorbed site. On the other hand, the effective local pH would suggest that the charged groups around the adsorbed disulfide bond are most probably positively charged, such as ammonium groups, consistent with our previous suggestion[7] that the adsorbed disulfide bond might be that of Cys61−Cys91, which is close to the N-terminus of the enzyme. In addition, this irreversibility was very dependent on the sweep rate, as shown in Figure 4b, where it can be seen that at low sweep rates (e.g., 1 V/s) the anodic wave was quite visible, and its peak height was close to that of the cathodic wave. This observation was again consistent with the earlier-mentioned argument that the anodic process involved the necessary movement of two thiol groups from two distinct mercury thiolate complexes to one adsorbed center in order for the disulfide bond to be regenerated. Without buffer present in the solution, any protonation/deprotonation process will result in an abrupt change of pH as well as the local charge distribution. Thus, the reduction products, namely the two RSH groups, could incur significant local charge disturbance so that their distance is no longer in the range necessary for the formation of a disulfide bond. The anodic wave's sensitivity to sweep rate was interpreted as being due to the fact that at lower sweep rates molecules had more time to rearrange, resulting in a fairly well-behaved voltammetric response in contrast to the case at high sweep rates. Here one should note that the cathodic wave was always well-defined, suggesting that the reduction of disulfide to the thiols is kinetically facile, and this might reflect the fact that whereas the thiols have a high localized negative charge density, the disulfide does not, making it less sensitive to such effects.

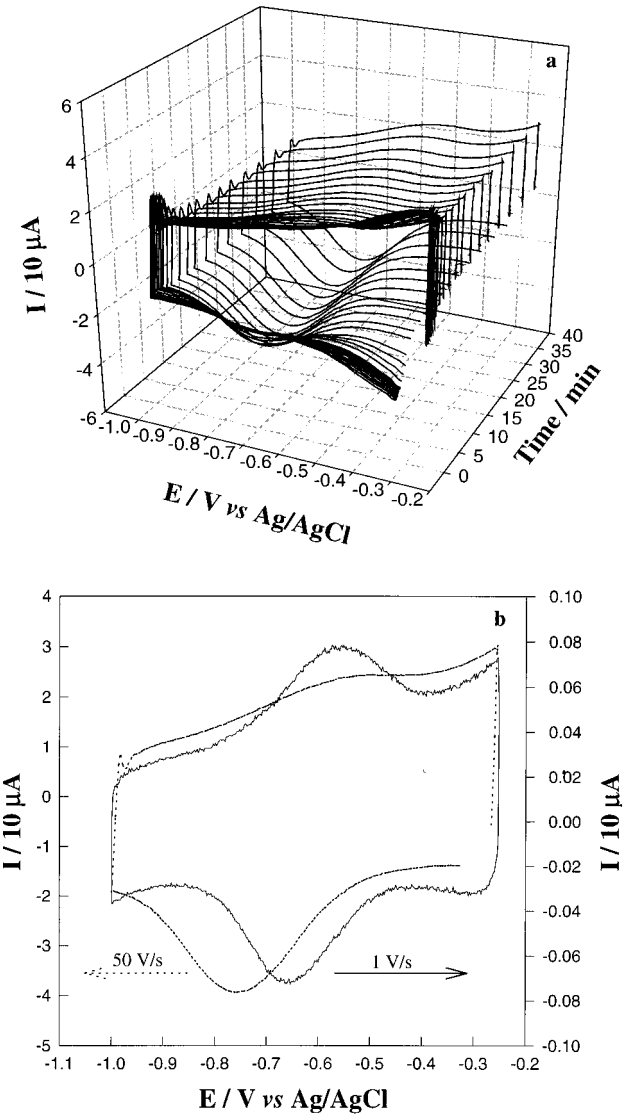

Figure 4. Cyclic voltammograms of PLA_2 adsorbed onto a mercury electrode surface in unbuffered 0.20 M KCl. Electrode area = 1.82 mm^2 and PLA_2 concentration = 0.09 μM. (a) Development of cyclic voltammograms vs adsorption time at a sweep rate of 50 V/s. (b) Steady state cyclic voltammograms at sweep rates of 50 and 1 V/s.

On the other hand, the proposed discrepancy of the interfacial and bulk pH (i) might, in part, account for the experimental result that the formal potential shifts 71 mV per unit of pH[7] in contrast to 59 mV as predicted by the Nernst equation; thus, one can determine their relationship as $pH_{interface} = 1.2pH_{bulk}$. (ii) The discrepancy is consistent with the above-mentioned effect of interfacial availability of protons on the reaction kinetics, as the interfacial proton concentration is lower than that in the bulk.

In short, the above dc cyclic voltammetric studies suggest that adsorption of PLA_2 onto a mercury electrode surface involves rather complex and coupled surface reactions. The reaction mechanism appears to depend on the specific conditions of the system, namely, the surface concentrations of adsorbed PLA_2 and free mercury, as well as the local pH buffering capacity. However, the overall reaction appears to be consistent with the mechanism of the cystine/cysteine system presented in the literature.

Electron Transfer Kinetics. To further understand the kinetics of the electron transfer process, we attempted to determine the values of the transfer coefficient, α, and the charge transfer rate constant, k. Laviron[10] has employed a mathematical

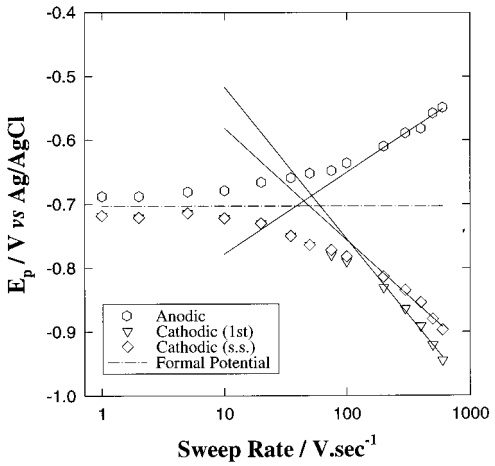

Figure 5. Semilogarithmic plots of the sweep rate effect on the peak potentials of the cathodic and anodic processes. Experimental conditions are the same as in Figure 2. Symbols are the experimental results; and the solid lines are the corresponding fits to eqs 10c and 10d.

approach to derive the formulations, which can be summarized below:

$$E_{p,c} = E^j - (RT/\alpha nF)\ln(\alpha/m) \quad (10a)$$

$$E_{p,a} = E^j - [RT/(1-\alpha)nF]\ln[(1-\alpha)/m] \quad (10b)$$

where $E_{p,c}$ and $E_{p,a}$ are the cathodic and anodic peak potentials, respectively; E^j is the formal potential, $(E_{p,c} + E_{p,a})/2$, $m = (RT/F)(k/n\upsilon)$, and R, T, F, and n have their usual significance. Here it should be noted that the above equations are only valid for a totally irreversible reaction. Experimentally, this can be very well approximated when the difference in peak potentials (ΔE_p) is $>200/n$ mV. By substituting m into eqs 10a and 10b, one can obtain

$$E_{p,c} = E^j - (RT/\alpha nF)\ln(\alpha nF/kRT) - (RT/\alpha nF)\ln \upsilon \quad (10c)$$

$$E_{p,a} = E^j + [RT/(1-\alpha)nF]\ln[(1-\alpha)nF/kRT] + [RT/(1-\alpha)nF]\ln \upsilon \quad (10d)$$

Plots of $E_{p,c}$ and $E_{p,a}$ vs ln υ yield two straight lines whose slopes (k_c and k_a) are equal to $-RT/\alpha nF$ and $RT/(1-\alpha)nF$, respectively. Therefore, one can determine the value of α from

$$\alpha = k_a/(k_a - k_c) \quad (11)$$

whereas the rate constant, k, can be determined from

$$k = \alpha nF\upsilon_c/RT = (1-\alpha)nF\upsilon_a/RT \quad (12)$$

where υ_c and υ_a are the cathodic and anodic sweep rates, respectively, when both $E_{p,c} - E^j$ and $E_{p,a} - E^j$ are equal to zero.

Figure 5 shows the sweep rate dependence of the peak potentials where one can see that at high sweep rate (>100 V/s) $\Delta E_p > 100$ mV. Thus, eqs 10c and 10d could be applied to the experimental data (recall that $n = 2$). Table 2 summarizes the results of α and k for the first cycle and steady state, under different pH conditions, where one can see that α's are in the range 0.35−0.50. This is consistent with the earlier observation that the shift of the anodic peak potential is more sensitive to the surface coverage than that of the cathodic wave. In addition, the values of α at steady state are somewhat larger than those for the first cycle, suggesting a slight increase in the symmetry of the energy barrier in the electron transfer process. This is consistent with the earlier observation that although there is incomplete reoxidation of RSH back to RSSR after the first cycle, on the subsequent scans the anodic and cathodic waves remain virtually unchanged, suggesting that the remaining sites exhibit rapid kinetics. On the other hand, the rate constants, k, were found to be virtually invariant between the first cycle and the steady state and of the order of 10^3 s^{-1}. It should be noted that as developed by Laviron, the theory is not strictly applicable to reactions involving proton transfers coupled to electron transfer as we appear to have in our case. However, the application of the theory provides a qualitative picture in terms of an "order of magnitude" estimate of the rate of electron transfer which was our intent.

TABLE 2: Electron Transfer Coefficient, α, and the Rate Constant, *k*, at Various Solution pH[a]

pH	α_1	α_2	k_1 (10^3 s^{-1})	k_2 (10^3 s^{-1})
7.5	0.45 ± 0.04	0.51 ± 0.06	1.6 ± 0.3	1.7 ± 0.1
8.6	0.35 ± 0.04	0.42 ± 0.05	1.8 ± 0.3	1.7 ± 0.1

[a] Subscripts 1 and 2 refer to the results of first cycle and steady state of the potential scans, respectively. Solution pH was adjusted with Tris/HCl buffers.

Electrical Properties of the PLA_2 Adsorbed Layer. To investigate the electrical properties of the adsorbed film of PLA_2, we carried out an ac cyclic voltammetric study at full coverage. For a system where both reactant and product are adsorbed on the electrode surface and their adsorption is mutually independent, it has been shown that the overall admittance can be expressed as[11]

$$Y = j\omega C_1 + \frac{j\omega C_O + j\omega C_R + {}^1/_2(\alpha_R C_O + \alpha_O C_R)(j-1)}{1 + {}^1/_2(\alpha_R + \alpha_O)(j+1) + {}^1/_2\alpha_R\alpha_{Oj}} \quad (13)$$

with

$$C_1 = A(\partial Q/\partial E)_{\Gamma_O,\Gamma_R}$$

$$C_0 = A(\partial Q/\partial \Gamma_O)_{E,\Gamma_R}(\partial \Gamma_O/\partial E)_{C_O,C_R}$$

$$C_R = A(\partial Q/\partial \Gamma_R)_{E,\Gamma_O}(\partial \Gamma_R/\partial E)_{C_O,C_R}$$

$$\alpha_O = (\partial \Gamma_O/\partial C_O)(2\omega/D_O)^{1/2}; \quad \alpha_R = (\partial \Gamma_R/\partial C_R)(2\omega/D_R)^{1/2} \quad (14)$$

where j is $(-1)^{1/2}$, A is the electrode area, $\omega = 2\pi f$ (f = ac frequency), Q is the charge, E is the applied electrode potential, Γ is the surface excess, C is the adsorbate solution concentration, and D is its diffusion coefficient. The subscripts O and R refer to the oxidized and reduced states, respectively. The overall admittance can be viewed as the combination of a capacitance C_1 in parallel with a kinetic impedance represented by the second term in (13). Consequently, the equivalent quadrature component of the electrode admittance can be recast as

$$Y'' = \omega C_1 + \omega C_f \quad (15)$$

where C_f represents the contribution involved in the faradaic process and is dependent upon C_O, C_R, α_O, and α_R. From eq 15, one would expect a linear dependency of the out-of-phase current (I'') on frequency, which can be expressed as

$$I'' = E''Y'' = E''\omega(C_1 + C_f) = 2\pi E'' f(C_1 + C_f) \quad (16)$$

where E'' is the amplitude of the ac signal. Although C_f is also a function of ω, the variations in ω were relative small so

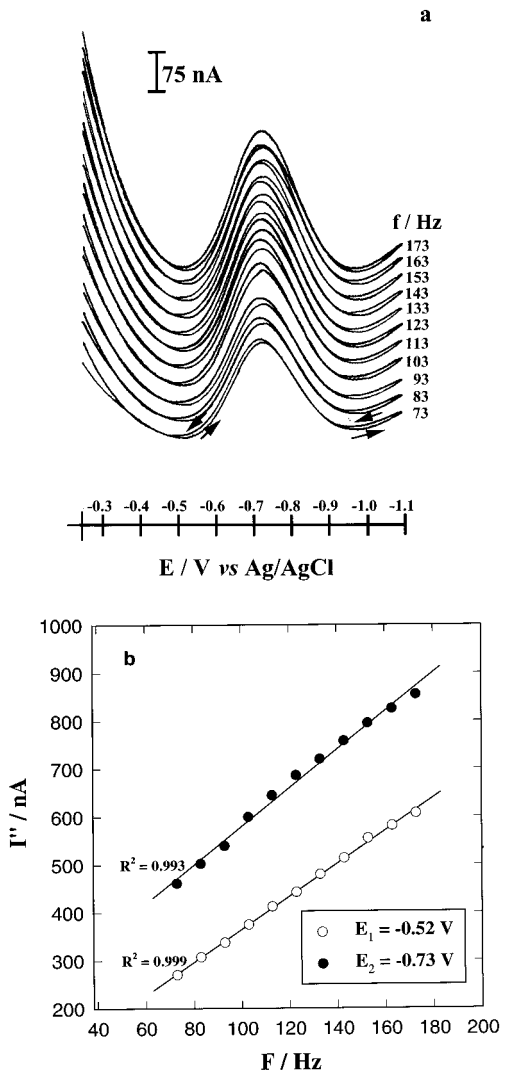

Figure 6. (a) The ac cyclic voltammograms of PLA_2 at the steady state of adsorption onto a mercury electrode surface. dc potential sweep rate is 10 mV/s and ac amplitude is 10 mV. Other experimental conditions are the same as in Figure 2. (b) Frequency dependence of the ac currents.

that the effect on C_f would also be ostensibly small, and we have assumed it to be negligible under our conditions.

Figure 6a shows the ac voltammograms of adsorbed PLA_2 at steady state, where one can see that there is a well-defined pseudocapacitance peak at about −0.73 V, which is very close to the dc formal potential. In addition, a minimum in the ac current is found at about −0.52 V, and this potential position is almost independent of the ac frequency. Figure 6b shows the frequency dependence of the ac currents at the peak (−0.73 V) and minimum (−0.52 V) positions, respectively, where excellent linear correlations ($R^2 > 0.99$) were obtained at both potentials. From the slopes, one can calculate the corresponding capacitance values. At $E_1 = -0.52$ V, where no faradaic process is taking place, $C_f = 0$; thus, the capacitance will be solely due to the purely capacitative part, namely, C_1. At $E = -0.73$ V where a faradaic process is proceeding, the calculated results will represent the combined contributions of C_1 and C_f. Table 3 summarizes the results for C_1 and C_f at various solution pH values, where it can be seen that C_1 is about 6 μF/cm^2, corresponding to an effective dielectric constant of about 6 by taking into account the adsorbed molecular dimensions.[7,12] One can also observe that, on the more negative side of the pseudocapacitance peak, there is another ac current minimum which corresponds to the reduced state of PLA_2, i.e., RSH, and this current is approximately equal to that at $E_2 = -0.52$ V, indicating that the overall interfacial dielectric properties of the adsorbed PLA_2 molecules were practically unchanged before and after the redox reaction. Although inferring structural information from capacitance measurements must be done with great care, what one can say is that based on these capacitance results, there appear to be no gross changes in the interfacial structure of adsorbed PLA_2 which is consistent with our previous suggestion that its overall molecular conformation is preserved during the adsorption and electron transfer processes.[7]

TABLE 3: Capacitance Composition of the PLA_2 Adsorbed Layer at Various Solution pH

pH	C_1 (μF/cm^2)	C_f (μF/cm^2)
7.5	6.6	0.6
8.6	6.0	1.0

Conclusions

Cyclic voltammetric studies were carried out in both ac and dc modes to study the interfacial interaction between adsorbed PLA_2 molecules and a mercury electrode surface. The surface reactions involving the adsorbed disulfide bond in PLA_2 were found to be quite complex with the reaction mechanism being dependent upon a variety of factors, among which the concentrations of surface mercury and PLA_2 and the surface pH buffering capacity were most influential. These findings were consistent with the nature of the surface reactions presented in (1)−(4). However, due to the very large molecular dimensions and amphiphilic nature of PLA_2, the corresponding surface reaction mechanism is more complex than that for the free cystine/cysteine system in terms of the adsorbed states of the thiolate complexes and consequently the predominating electron transfer pathways. This indicates that the interfacial microstructure can play a key factor in determining the surface behavior of adsorbed molecules. Studies of electron transfer kinetics showed that the transfer coefficient (α) was somewhat less than 0.50 and that the rate constant (k) was of the order of 10^3 s^{-1}. The ac cyclic voltammetric studies showed that the capacitance of the adsorbed PLA_2 layer was around 6 μF/cm^2 and that the faradaic component of the interfacial capacitance was about 1 μF/cm^2.

We are currently developing an approach for evaluating the interfacial enzymatic activity of PLA_2 on phospholipid monolayers on a mercury electrode surface. The results presented here are an essential first step to the understanding of the interfacial behavior of the enzyme and provide insight into the hydrolytic effect of the enzyme on these lipid assemblies. These studies are currently underway and will be reported elsewhere.

Acknowledgment. This work was supported by the National Science Foundation through Grant DMR-9107116. The authors acknowledge the assistance of Mr. Y. Liu in data collection.

References and Notes

(1) (a) Widrig, C. A.; Chung, C.; Porter, M. D. *J. Electroanal. Chem.* **1991**, *310* (1−2), 335−359. (b) Walczak, M. M.; Popenoe, D. D.; Deinhammer, R. S.; Lamp, B. D.; Chung, C.; Porter, M. D. *Langmuir* **1991**, *7*, 2687−2693. (c) He, Z.; Bhattacharyya, S.; Cleland, W. E.; Hussey, C. L. *J. Electroanal. Chem.* **1995**, *397*, 305−310. (d) Mrksich, M.; Sigal, G. B.; Whitesides, G. M. *Langmuir* **1995**, *11*, 4383−4385.

(2) (a) Watanabe, T.; Maeda, H. *J. Phys. Chem.* **1989**, *93*, 3258−60. (b) Bryant, M. A.; Pemberton, J. E. *J. Am. Chem. Soc.* **1991**, *113*, 3629−37. (c) Curtin, L. S.; Peck, S. R.; Tender, L. M.; Murray, R. W.; Rowe, G. K.; Creager, S. E. *Anal. Chem.* **1993**, *65*, 386−92.

(3) (a) Magno, F.; Bontempelli, G.; Pilloni, G. *J. Electroanal. Chem. Interfacial Electrochem.* **1971**, *30*, 375−83. (b) Reddy, S. J.; Krishnan, V. R. *Anal. Chem. Symp. Ser.* **1980**, *2*, 155−63.

(4) (a) Donahue, J. J.; Olver, J. W. *Anal. Chem*. **1969**, *41*, 753−757. (b) Trijuque, J.; Sanz, C.; Monleon, C.; Vicente, F. *J. Electroanal. Chem*. **1988**, *251*, 173−182. (c) Pardo, M.; Angulo, M.; MarinGalvin, R.; Rodriguez Mellado, J. M. *Electrochim. Acta* **1996**, *41*, 133−139.

(5) (a) Lecompte, M. F.; Miller, I. R. *Biochemistry* **1980**, 3439−3446. (b) Lecompte, M. F.; Bouix, G.; Mann, K. G. *J. Biol. Chem*. **1994**, *269*, 1905−1910. (c) Lecompte, M. F.; Duplan, H. In *Proteins at Interfaces II: Fundamentals and Applications*; Horbett, T. A., Brash, J. L., Eds.; American Chemical Society: Washington, DC, 1995; pp 519−532.

(6) (a) Miller, I. R.; Teva, J. *J. Electroanal. Chem.* **1972**, *36*, 157−166. (b) Stankovich, M. T.; Bard, A. J *Ibid*. **1977**, *75*, 487−505. (c) Forsman, U. *Ibid*. **1983**, *152*, 241−254. (d) Matsushita, F.; Miyaoka, S.; Ikeda, T.; Senda, M. *Anal. Sci.* **1991**, *7* (Suppl), 1685−1688. (e) Heyrovsky, M.; Mader, P.; Veselç, V.; Fedurco, M. *J. Electroanal. Chem*. **1994**, *369*, 53−70. (f) Vavricka, S.; Heyrovsky, M. *Ibid*. **1994**, *375*, 371−373. (g) Ralph, T. R.; Hitchman, M. L.; Millington, J. P.; Walsh, F. C. *Ibid*. **1994**, *375*, 1−15. (h) Ralph, T. R.; Hitchman, M. L.; Millington, J. P.; Walsh, F. C. *Ibid.* **1994**, *375*, 17−27.

(7) Chen, S.; Abruña, H. D. *J. Phys. Chem*. **1995**, *99*, 17235−17243.

(8) Grahame, D. C. *Chem. Rev*. **1947**, *41*, 441.

(9) *Handbook of Physics and Chemistry*, 69th ed.; Weast, R. C., Ed.; CRC Press: Boca Raton, FL, 1988−1989; p F-166.

(10) Laviron, E. *J. Electroanal. Chem*. **1979**, *101*, 19−28.

(11) Moreira, H.; De Levie, R. *J. Electroanal. Chem*. **1972**, *35*, 103.

(12) Waite, M. *Handbook of Lipid Research, the Phospholipase*; Plenum Press: New York, 1987; p 4.